American Journal of Pathology, Vol. 168, No. 5, May 2006

DOI: 10.2353/ajpath.2006.050847

Tumorigenesis and Neoplastic Progression

Rapid Development of Salivary Gland Carcinomas upon Conditional Expression of K-*ras* Driven by the Cytokeratin 5 Promoter

Ana R. Raimondi, Lynn Vitale-Cross, Panomwat Amornphimoltham, J. Silvio Gutkind, and Alfredo Molinolo

From the Oral and Pharyngeal Cancer Branch, National Institute of Dental Research, National Institutes of Health, Bethesda, Maryland

We have used a recently described model in which a *ras* oncogene is expressed in cytokeratin 5 (K5)-expressing cells on doxycycline administration to explore the effects of this oncogene in salivary glands of adult mice. Inducible expression of a mutated K-*ras* gene under the control of the K5 promoter led to the development of hyperplastic and dysplastic epithelial lesions and carcinomas, with an incidence of 100% and a minimum latency of a week. All major salivary glands were affected, as well as a set of previously undescribed buccal accessory salivary glands located on the apex of the masseter muscle, close to the oral angle. The tumors appear to arise from the cytokeratin 5-positive basal cell compartment. Myoepithelial cells participated in the hyperplasias but not in carcinomas, because the tumors are negative for smooth muscle actin. Carcinomas did not accumulate immunoreactive p53 but are positive for p63, as assayed by immunohistochemistry using an antibody against the N terminus of ΔN p63, a splice variant of p63 that can inhibit p53 transcriptional activity. In this study, we provide evidence that the *ras* oncogene, targeted to a specifically sensitive cell compartment within the salivary glands, can trigger a series of event that are sufficient for full carcinogenesis. ***(Am J Pathol 2006, 168:1654–1665; DOI: 10.2353/ajpath.2006.050847)***

Malignant tumors of the salivary glands are a relatively rare oral neoplasia, comprising <0.5% of all malignancies combined and ~5% of malignancies of the head and neck region.[1] They have a special status in human neoplasia, because they exhibit the most complex histopathology of any tumor type, and for this reason they represent a morphologically diverse group of tumors.[2] This complexity is reflected in the current classification schemes that are mostly based in histological parameters,[3] although efforts have been made to correlate this growing list of tumors with their biological behavior.[4] This histological approach to classification, although useful for other tumor types, has failed to satisfy the needs of those directly involved in the treatment of salivary gland tumors,[1] who often fail to see in these complex diagnoses a useful guide for treatment standardization. This problem, largely reflecting our lack of understanding of the possible correlation between histological patterns and tumor prognosis, has been the focus of extensive review.[2]

Several approaches, including the use of chemicals,[5] viruses,[6] radioactive isotopes,[7] and genetically engineered animals (reviewed by Dardick[8]), have been used to developed experimental models that may help understand the carcinogenic process in salivary glands. Compared to other approaches, transgenic mouse models have the advantage of allowing a refined molecular dissection of each of the steps involved in tumor development and progression, because the variability within a given model is generally low and the carcinogenic events proceed through homogeneous steps and similar histological changes. Several of the available models have taken advantage of the mouse mammary tumor virus (MMTV) promoter to target the expression of different oncogenes to salivary and mammary glands. However, the resulting salivary gland phenotypes are not homogeneous across different models and have been less characterized than, for example, mammary gland tumors, the induction of which has been in most studies the original purpose of the experimental design.

In this regard, a wide spectrum of premalignant and malignant changes have been described in the sali-

Supported by the Intramural Research Program of the National Institute of Dental and Craniofacial Research, National Institutes of Health.

Accepted for publication January 10, 2006.

Address reprint requests to Alfredo Molinolo, Oral and Pharyngeal Cancer Branch, NIDCR, National Institutes of Health, 30 Convent Drive, Building 30, Room 213, Bethesda, Maryland 20892-4340. E-mail: amolinol@mail.nih.gov.

vary glands of transgenic mice in which the MMTV promoter drives the expression of different oncogenes, though with a variable incidence rate and usually a prolonged latency. For example very few transgenic mice in which an *int-1* allele resembling those found in virus-induced tumors is expressed from the MMTV long terminal repeat developed salivary adenocarcinomas.[9] Incomplete differentiation and dysplastic changes in all glands, as well as poorly differentiated adenocarcinomas apparently arising from the parotid gland, have been reported in the MMTV-int-3 mouse,[10] and well circumscribed salivary gland adenocarcinomas developed with a low incidence (3 out of 62 mice) in the MMTV-Fgf8 transgenic mouse.[11] On the other hand, 22% of MMTV-v-Ha-*ras* animals developed acinic cell carcinomas only in the parotid gland at 73 to 150 days of age.[12] This limited effect of *ras* is surprising because expression of the activated form of genes for the Ras family of GTPases, H-Ras, K-Ras, and N-Ras has been associated with the pathogenesis of a wide variety of human tumors, including salivary gland neoplasm.[13–16] Indeed, the H-*ras* gene has been found mutated in 35% of the salivary gland pleomorphic adenomas[14] and in adenocarcinomas of the parotid glands, albeit with a slight lower incidence (23%).[17]

Leaky transgenic expression of oncogenes in salivary gland tissues when using a variety of promoters can also result in a low incidence of salivary gland tumors. For example, animals expressing the human H-*ras* oncogene from the murine whey acidic protein promoter develop salivary gland adenocarcinomas in male animals after several months.[18] Expression of a similar H-*ras* oncogene driven by the human prostate-specific antigen promoter leads to the development of salivary gland tumors of possible ductal origin, ranging from well differentiated adenocarcinomas to anaplastic carcinomas, in <50% of the animals older than 11 months.[19] If instead a promoter from the neonatal submandibular gland secretory protein b gene is used to express the SV40 large T antigen specifically in salivary glands, at 1 month of age animals develop duct luminal cell hyperplasias that progress to dysplasia within 3 to 4 months and severe dysplasia and *in situ* carcinoma within 4 to 6 months. Submandibular gland adenocarcinomas originating from the intercalated ducts also develop in about half of the male mice by 12 months of age.[8]

In this study, we took advantage of the observation that salivary glands express cytokeratin 5 (K5) in ductal epithelia and the availability of a recently described inducible animal model in which a *ras* oncogene is expressed in K5-expressing cells on doxycycline administration to explore the biological consequences of the conditional expression of this oncogene in salivary glands in adult mice. We found that, when a mutated K-*ras* gene was conditionally expressed in the salivary glands under the control of the K5 promoter, it induces hyperplastic and dysplastic lesions and carcinomas, with an incidence of 100% of the animals and a minimum latency as short as 1 week. Indeed, we provide evidence that the *ras* oncogene, when targeted to a specifically sensitive cell compartment within the salivary glands, can trigger a series of event that are sufficient for full carcinogenesis.

Materials and Methods

Transgenic Mice

The K5-*rTA* (K5-*tet*-on), *tet-ras* (K-*ras*4bG12D), and *tetO*-LacZ transgenic mice have been previously described.[20] Doxycycline was administered via the drinking water at a concentration of 1 g/L to a total of 24 animals of 21 days of age. A similar number of wild-type animals as well as transgenic mice not receiving doxycycline treatment were used as controls. All mice were examined daily.

Tissue Preparation, Histology, and Immunohistochemistry

K5-*tet*-on/*tet*-o-*ras* mice as well as control animals were injected with 5-bromo-2′-deoxyuridine (BrdU; Sigma-Aldrich Corp., St. Louis, MO) and euthanized with CO_2 after 2 hours. All major salivary glands were carefully dissected. To better assess the location and microscopic features of the accessory buccal glands, samples, including skin and buccal mucosa from the oral angle, were obtained from several wild-type animals. All tissues were fixed overnight in buffered 4% paraformaldehyde, transferred to 95% ethanol, and embedded in paraffin. Five-micron sections were cut and stained with hematoxylin and eosin or used for immunocytochemical studies. Alcian blue staining was used in selected buccal salivary gland sections to provide a better contrast for illustration purposes. To ascertain the expression of the promoter, double transgenic mice expressing the β-galactosidase gene under the control of the K5-*tet*-on system were euthanized with CO_2. Cryostat sections were obtained from frozen salivary gland samples and fixed in 4% buffered paraformaldehyde 1 hour at 4°C. For immunocytochemical studies, the following antibodies were used: rabbit polyclonal antibody against mouse keratin 5 (Covance, Denver, PA) at 1:500 dilution; mouse *p63* monoclonal antibody (4A4, sc-8431 Santa Cruz Biotechnology Inc., Santa Cruz, CA), raised against amino acids 1 to 205 mapping at the N terminus of ΔN *p63* of human origin, at 1:100 dilution; rabbit p53 monoclonal antibody (Cell Signaling Technology, Beverly, MA) at 1:40 dilution; rabbit polyclonal antibody against smooth muscle actin (RB-9010; Lab Vision, NeoMarkers and Lab Vision Corporation, Fremont, CA) at dilution 1:100; and rat anti-BrdU monoclonal antibody (Accurate Chemical, Westbury, NY) at 1:10 dilution. Secondary antibodies were conjugated with biotin (Vector, Burlingame, CA) and diluted 1:400. All antibodies were diluted in 2.5% bovine serum albumin (BSA, Sigma, St. Louis, MO) in phosphate-buffered saline (PBS). Cryostat sections were washed with PBS and processed for β-galactosidase staining.[21] The tissues slides were dewaxed in SafeClear II (Fisher), hydrated through graded alcohols, and immersed in 3% hydrogen peroxide in PBS for 30 minutes to

quench the endogenous peroxidase. After washing in distilled water, antigen retrieval was performed with 10 mmol/L citric acid in a microwave for 20 minutes (2 minutes at 100% power and 18 minutes at 10% power). Slides were allowed to cool for 30 minutes at room temperature, rinsed thoroughly with distilled water and PBS, and incubated in blocking solution (2.5% BSA in PBS) for 30 minutes at room temperature. Excess solution was discarded, and the sections were incubated with the primary antibody diluted in blocking solution at 4°C overnight. After washing with PBS, the slides were sequentially incubated with the biotinylated secondary antibody (1:400; Vector, Burlingame, CA) for 1 hour, followed by the avidin-biotin complex method (Vector Stain Elite, ABC kit; Vector) for 30 minutes at room temperature. For BrdU staining the slides were dewaxed as indicated, incubated with 2 N HCl at 37°C for 1 hour, and washed with water and PBS and then finally with 2.5% BSA in PBS (PBS-BSA). After discarding the PBS-BSA solution, the slides were incubated with the anti-BrdU antibody at 4°C overnight. The secondary antibody used was anti-rat immunoglobulins (Vector), diluted 1:400 in PBS-BSA at room temperature for 30–45 minutes. The slides were washed and developed in 3,3′-diaminobenzidine (FASTDAB tablet; Sigma) under microscopic control. The reaction was stopped in tap water, and the tissues were counterstained with Mayer's hematoxylin, dehydrated, and mounted.

β-Galactosidase Staining

Briefly the sections were rinsed in PBS and washed for 15 minutes in rinse buffer (21). They were then incubated overnight at 37°C in X-gal staining solution (1 mg/ml 5-bromo-4-chloro-3-indolyl-β-galactopyranoside, 10 mmol/L $K_3Fe(CN)_6$, 10 mmol/L $K_4Fe(CN)_6$ and 1.2 mmol/L $MgCl_2$ in PBS). After the reaction was fully developed, the sections were postfixed in 4% paraformaldehyde and counterstained with Nuclear Fast Red. All stained slides were scanned at 200× using an Aperio T3 Scanscope (Aperio Technologies, Inc., Vista, CA) to produce high definition images. For selected samples, several partially overlapping high definition images were taken with a total magnification of 160× using a real-time Retiga 1300 digital camera with the QImaging Pro software (MVIA, Inc., Monaca, PA). The images were then stitched together using the PanaVue Image Assembler Software (PanaVue Co., Quebec City, QC, Canada). Dysplasias were defined as any intraepithelial, noninvasive morphological change carrying any atypical cytological markers that are widely accepted to precede invasive carcinomas.[22]

Results

Gross Anatomy

Mice expressing the K-*ras* oncogene under the control of the K5-*tet*-on-inducible system developed a wide range of proliferative lesions in the skin and other squamous epithelia.[20] Of note, these mice also exhibited a complex salivary gland phenotype, presenting visible lesions in the major and accessory buccal salivary glands (Figure 1) after only 1 week of doxycycline treatment (Table 1). A swollen, irregular neck area could be easily observed in live animals; at palpation, the glands felt hard and irregular. At necropsy the salivary glands looked enlarged and distorted, frequently weighing up to three times their normal weight (Figure 1, A–C). Bilateral tumor-looking structures were also seen on the masseter muscles ranging from 1 to 3 mm in diameter (Figure 1A). These tumors seem to have originated in small, microscopic mixed accessory salivary glands located close to the superficial muscular layer, which is close to the buccal mucosa, in the oral angle, and close to the border between the skin and the buccal mucosa (Figure 1D). These glands differed in histology and location from the extraorbital lacrimal glands, which were not affected by the carcinogenic process, and from the sebaceous glands located in the angles of the mouth that open directly to the mucosal surface.[23] No gross alterations were evident in untreated transgenic or wild-type animals.

Salivary Gland Phenotype

Submaxillary glands were affected in all cases, displaying the wider range of pathological alterations. Epithelial proliferation ranged from hyperplasia of the small secretory ducts, in the form of adenosis (Figure 3, lower inset), to solid hyperplasia and squamous metaplasia of the larger ducts. The acini did not seem to be involved in the proliferative lesions. Sublingual and parotid glands were less affected, and the lesions progressed from ductal, intralobular, and extralobular structures (Figures 2–4).

During the development of the phenotype, the excretory interlobular ducts of both submaxillary and sublingual glands showed immature squamous metaplasia in the early lesions, with cytological features of dysplasia, but these lesions did not tend to progress. The proliferation seems to arise from a basal cell compartment, and the dysplastic features were present from the very beginning. Within the lobular compartment the early stages of the phenotype were characterized only by epithelial proliferation; in later stages, particularly the submaxillary glands, there was a complex phenotype in which hyperplasia, squamous metaplasia, and dysplasia of the intercalated and secretory ducts were associated with fibroblastic proliferation and fibrosis (Figures 2 and 3). In certain areas, the general structure of the gland showed a fibroadenomatous-like picture (Figure 3, upper inset). Adenosis, with proliferation of small tubular structures surrounded by loose connective tissue, was also seen (Figure 3B, lower inset). Some of the metaplastic/dysplastic ducts showed early progression into invasive carcinomas, and within a few days, overt moderately to poorly differentiated squamous carcinomas developed that infiltrated the gland and surrounding tissues (Figure 4). In submaxillary and sublingual glands, as well as in the accessory buccal glands, invasive carcinomas lesions were frequently multifocal (Figure 4, B and C).

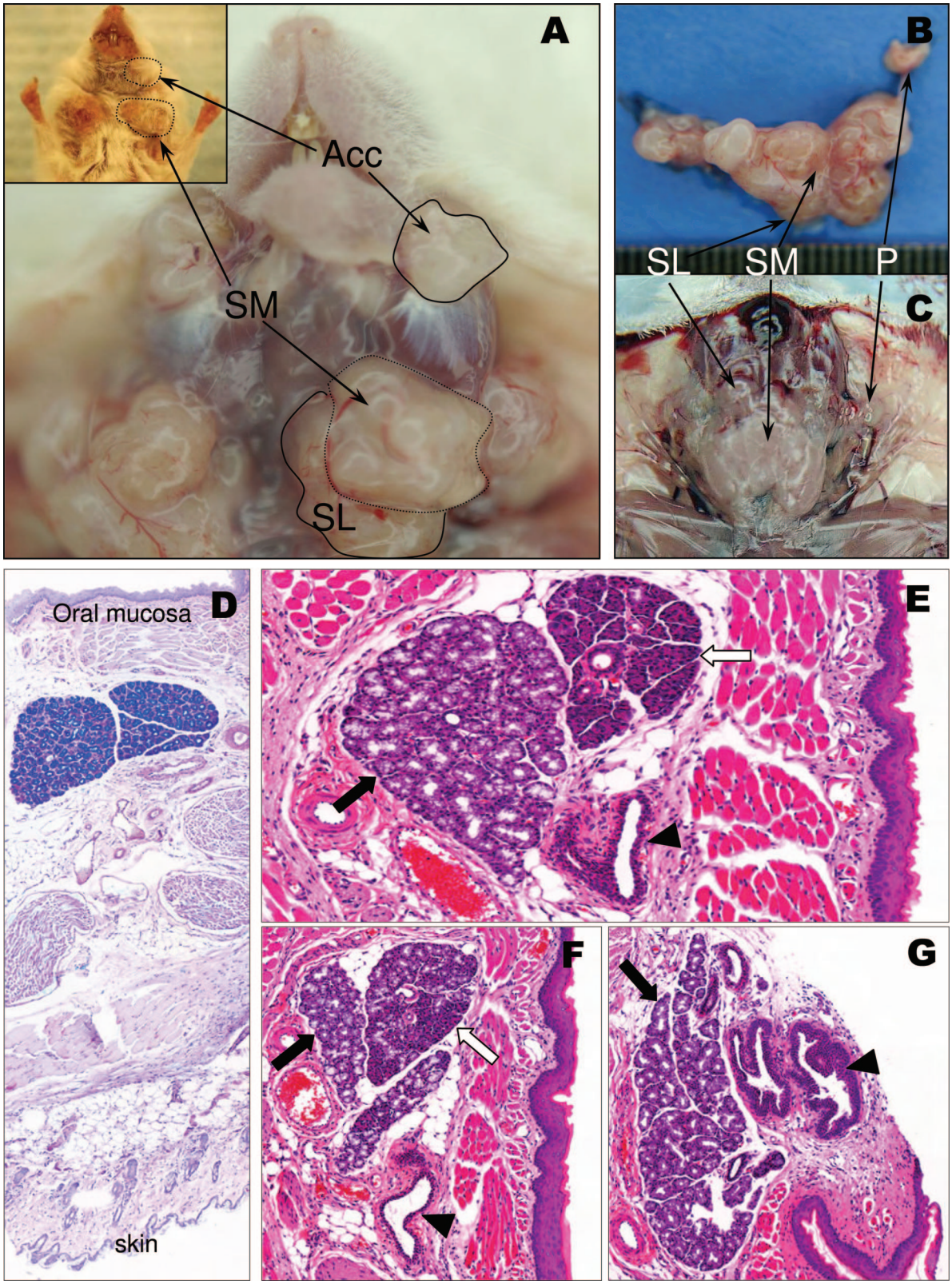

Figure 1. A: Gross anatomy of the salivary glands in a K5-*tet*-on/*tet*-o-*ras* animal. All glands are grossly distorted and enlarged showing a multinodular surface (SM: submaxillary, SL: sublingual). The accessory buccal glands (Acc) are also enlarged. The **inset** shows the glands already visible as tumor-like structures protruding through the neck skin. The abnormal gross anatomy is better depicted in the dissected gland (**B**) surface (SM: submaxillary, SL: sublingual, P: parotid); **C:** Relatively flat end even surface of normal salivary glands for comparison. **D–G:** Normal histology of the accessory salivary glands. These are microscopic mixed, mucous, and serous glands (**inset**, ductal structure), inconspicuous unless enlarged, located beneath the superficial muscular layer close to the buccal mucosa. **D:** Location of the glands in relation to the oral mucosa and the skin (Alcian Blue, 64×). **E:** Serous (**white arrow**) and mucinous (**black arrow**) lobules are separated at this level by a thin connective wall. In deeper sections both components coalesce (**F**), and the serous component disappears in even deeper sections (**G**). Excretory ducts are indicated by an **arrowhead**. (Different amplifications of pictures taken at 10× are shown.)

Table 1. Salivary Glands Phenotype of K5-*tet*-on/*tet*-o-K-*ras* Mice

Mouse no.	Sex	Doxycycline treatment (days)	Diagnostic	SM	SL	P	Accessory glands
1	F	6	Hyperplasia	Yes	–	–	nd
2	F	7	Adenosis	Yes	Yes	Yes	nd
3	F	7	SCC	Yes	–	–	nd
4	M	7	Hyperplasia	Yes	Yes	–	nd
5	M	7	SCC	Yes	–	–	nd
6	M	7	Hyperplasia/SCC	Yes	Yes	–	nd
7	M	7	Hyperplasia	Yes	–	–	nd
8	M	7	Hyperplasia/SCC	Yes	–	–	nd
9	M	7	Hyperplasia/fibrosis/SCC	Yes	–	–	nd
10	F	7	Hyperplasia/fibrosis	Yes	–	–	nd
11	F	7	Hyperplasia	Yes	Yes	Yes	Yes
12	F	10	Hyperplasia/SCC	Yes	Yes	–	Yes
13	M	11	Hyperplasia/SCC	Yes	Yes	–	–
14	M	14	Hyperplasia	Yes	Yes	Yes	–
15	M	15	Hyperplasia	Yes	Yes	–	nd
16	M	15	Hyperplasia/SCC	Yes	–	–	nd
17	M	15	Adenosis/hyerplasia	Yes	Yes	Yes	–
18	M	15	Adenosis/hyperplasia	Yes	Yes	–	–
19	M	23	Hyperplasia	Yes	Yes	Yes	–
20	F	28	Hyperplasia	Yes	Yes	Yes	–
21	M	29	Hyperplasia	Yes	Yes	–	Yes
22	M	30	Hyperplasia/SCC	Yes	Yes	–	Yes
23	M	30	Hyperplasia/SCC	–	–	–	Yes
24	F	32	Adenosis/hyperplasia	Yes	–	–	–

Doxycycline (RPI) was administrated via the drinking water at a concentration of 1g/L to 24 animals of 21 days of age. nd, not done. SM, submaxillary; SL, sublingual; SCC, squamous cell carcinoma; P, parotid.

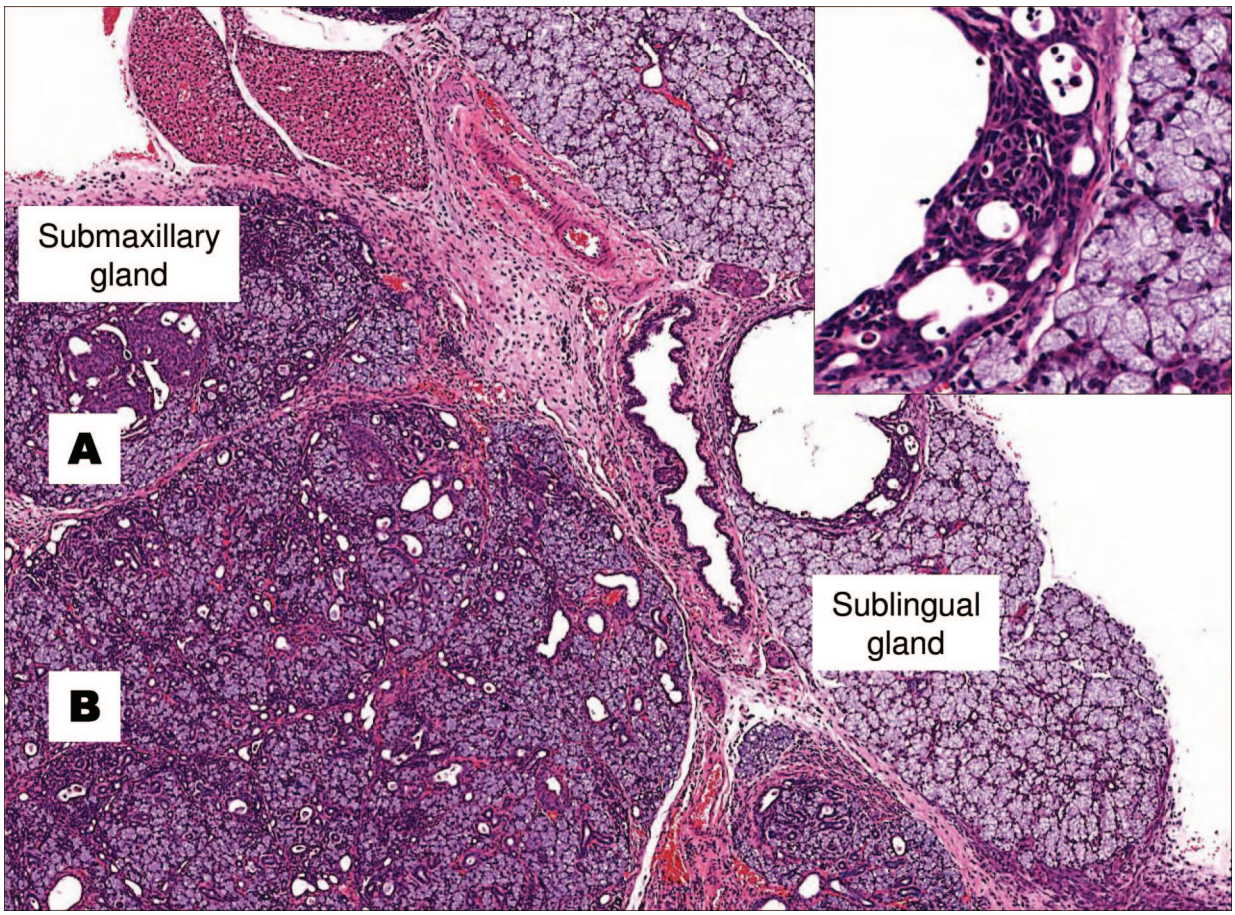

Figure 2. Dysplastic changes with solid squamous metaplastic proliferation (**A**) and adenosis (**B**) are evident in the submaxillary gland. The parenchyma of the sublingual gland seems unaffected, but the extralobular ducts show focal intraductal cribiform proliferation (**inset**). Magnifications: ×40 and ×100 (**inset**).

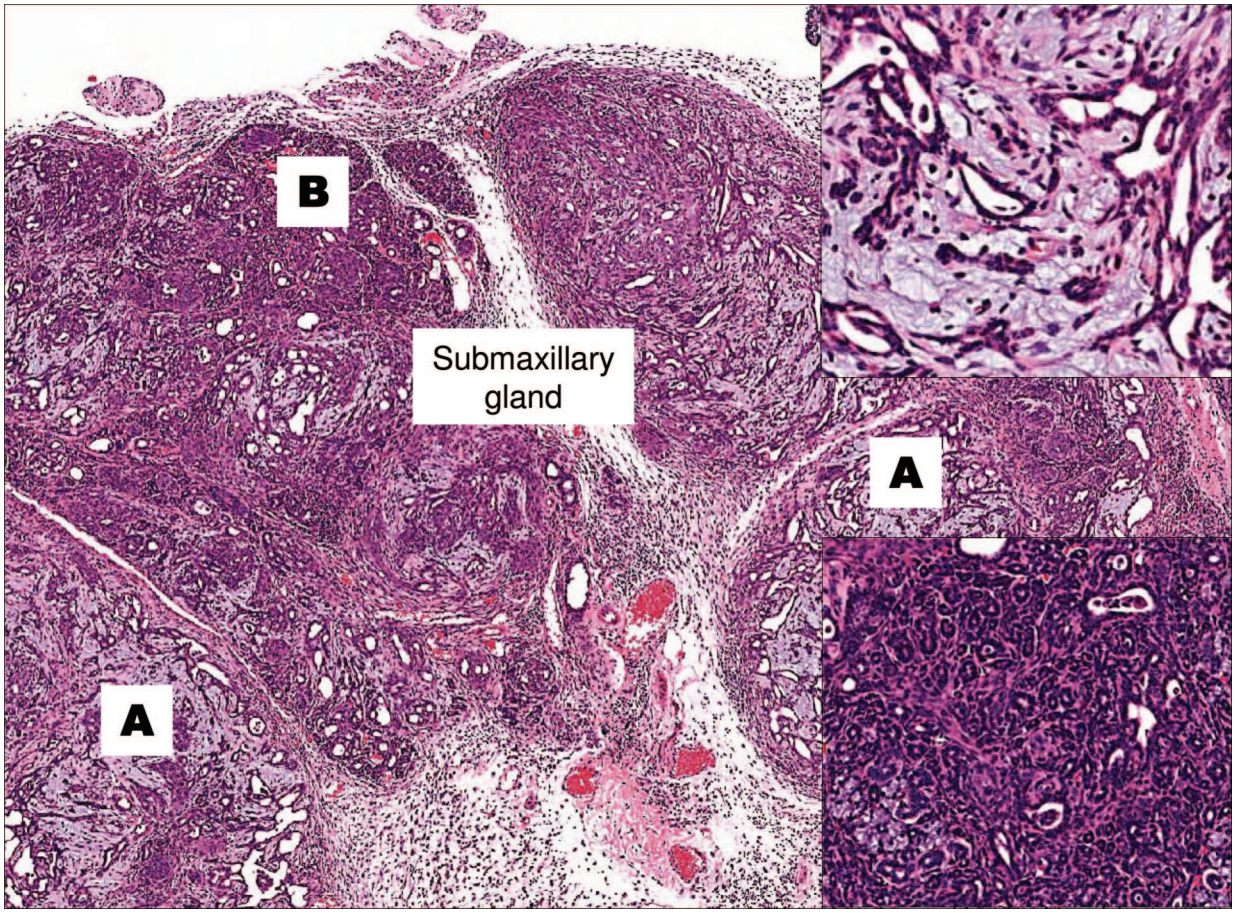

Figure 3. Advanced dysplastic changes with fibroadenoma-like changes (**A** and **inset**, upper right corner) and complex adenosis (**B** and **inset**, lower right corner). Few mononuclear cells can be seen in the stroma. These are a later development in the evolution of the process; no infiltrates are seen in early time points. Magnifications: ×40 and ×100 (**insets**).

Sublingual gland lesions developed later than those of the submaxillary gland and consisted of hyperplasias, squamous metaplasias/dysplasias, and invasive carcinomas. Adenosis of small ducts with the associated stromal proliferation and fibrosis, so frequently observed in submaxillary, were not seen in this gland. One of the distinctive features of these lesions was the early transformation; even relatively small groups of proliferating cells had already acquired the histological features of nonkeratinizing squamous cell carcinomas and were infiltrating the surrounding parenchyma (Figure 4). The majority of these carcinomas, frequently spindle-shaped, were moderately or poorly differentiated tumors (Figure 4, D and E), composed of densely packed chords of neoplastic cells with a high mitotic index and abnormal mitotic figures. Of the three major salivary glands, the parotids were the least frequently affected, usually starting late as compared with the other glands. These lesions were mainly characterized by scattered squamous metaplasia, hyperplasia, and dysplasia of the small intralobular ducts. Accordingly, progression into invasive carcinoma was also less frequent and a late event as well. An interesting feature of the general phenotype was the observation of lesions in a set of buccal accessory salivary glands located anatomically on the apex of the masseter muscle, close to the oral angle. Although these glands are not normally visible at necropsy, they became grossly evident when they developed proliferative lesions. Histologically they are mixed serous/mucinous glands in the submucosa of the mouth, seeming to arise from two independent components and draining into the oral cavity through a short and wide duct (Figure 1). Figure 5 depicts a low magnification image of the affected glands in which the whole spectrum of lesions, ranging from hyperplasia to squamous carcinoma, can be recognized. Most animals with accessory gland lesions also had lesions of the major salivary glands. Metastasis to regional cervical lymph nodes was observed in two cases (Figure 4F). It was not possible to determine from which gland they arose, but in both cases the submaxillary gland had the most advanced alterations. Untreated double transgenic K5-*tet*-on/*tet*-*ras*, as well as wild-type mice, were histologically normal. Persistence of salivary gland tumors as well as skin lesions, part of the general phenotype already described,[20] were observed in four K5-*tet*-on/*tet*-o-*ras* animals necropsied a month after stopping the doxycycline treatment. These preliminary results of a set of ongoing experiments suggest that the malignant salivary phenotype continue to progress despite suspension of the doxycycline treatment.

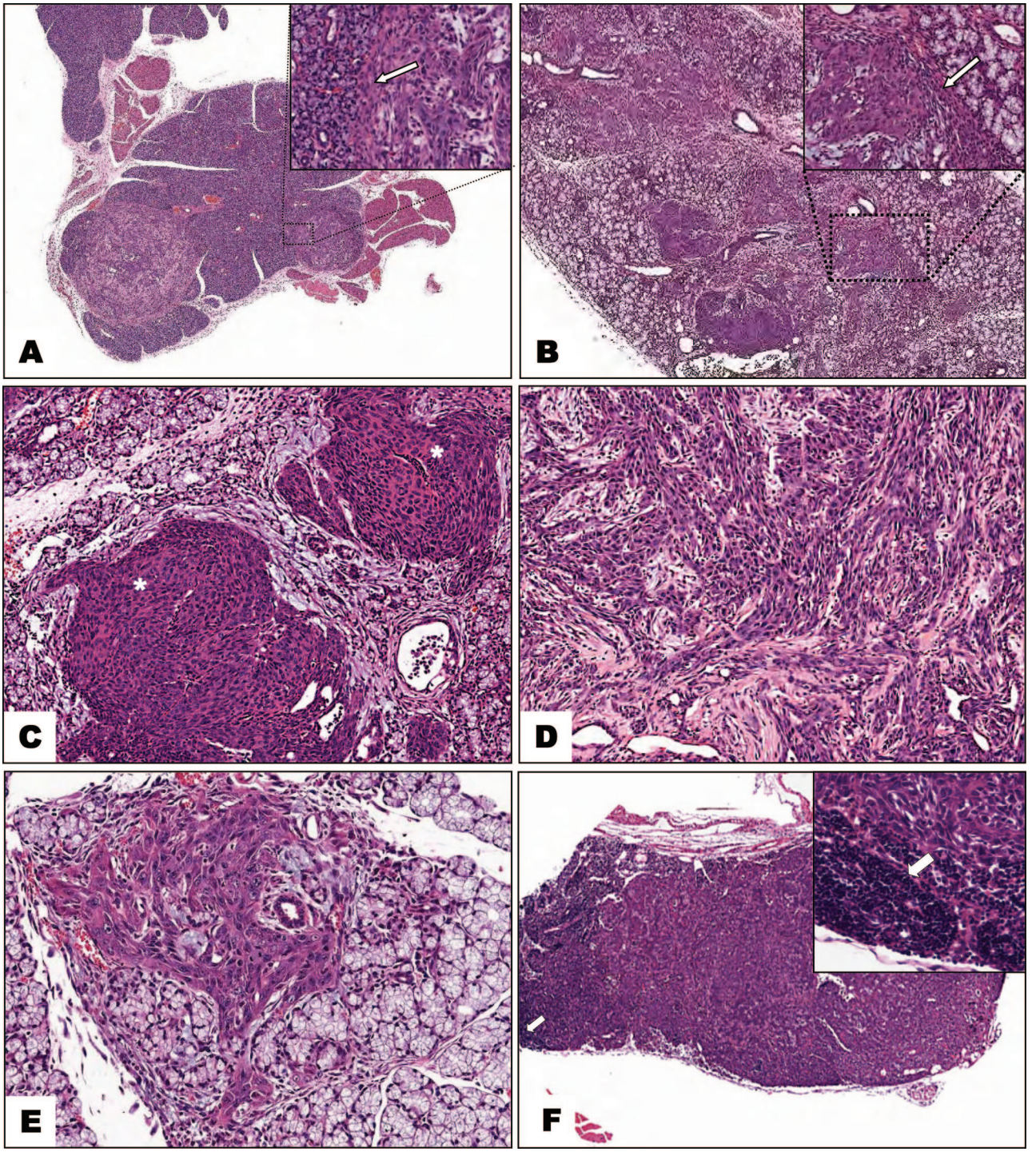

Figure 4. A: This multifocal squamous cell carcinoma arises in an otherwise unaffected submaxillary gland; no signs of hyperplasia or dysplasia are observed. The **inset** shows a distinct limit between neoplasia and normal tissue (**arrow**). **B:** Multifocal spindle-cell carcinomas in a sublingual gland arising from ductal structures; the **inset** depicts the border between the carcinoma and the normal tissue; a fibrous pseudocapsule with inflammatory mononuclear cells is seen (**arrow**). **C:** Moderately differentiated multifocal squamous cell carcinoma arising in a submaxillary gland; the tumors form solid masses that infiltrate the surrounding stroma. Distorted mucous acini are seen in the periphery. **D:** Infiltrating spindle-shaped carcinoma, with a desmoplastic stroma. **E:** Early carcinoma arising in a dysplastic sublingual gland. Note that, although the lesion is small, all of the cells display malignant features; a rapid transition to invasion characterized these tumors, with no evident dysplasias. **F:** Metastatic squamous cell carcinoma in a cervical lymph node; the **arrows** indicate remnants of the lymph node parenchyma. Magnifications: ×20 (**A**); ×30 (**B**); ×45 (**C–F**); and ×100 (**insets**).

Gene Expression

Double transgenic mice expressing the β-galactosidase gene under the control of the K5-*tet*-on system revealed β-galactosidase activity in the ducts of the salivary glands after administration of doxycycline, confirming the specific expression of the K5 promoter in the salivary glands (Figure 6A). Indeed, immunocytochemistry for K5 revealed staining

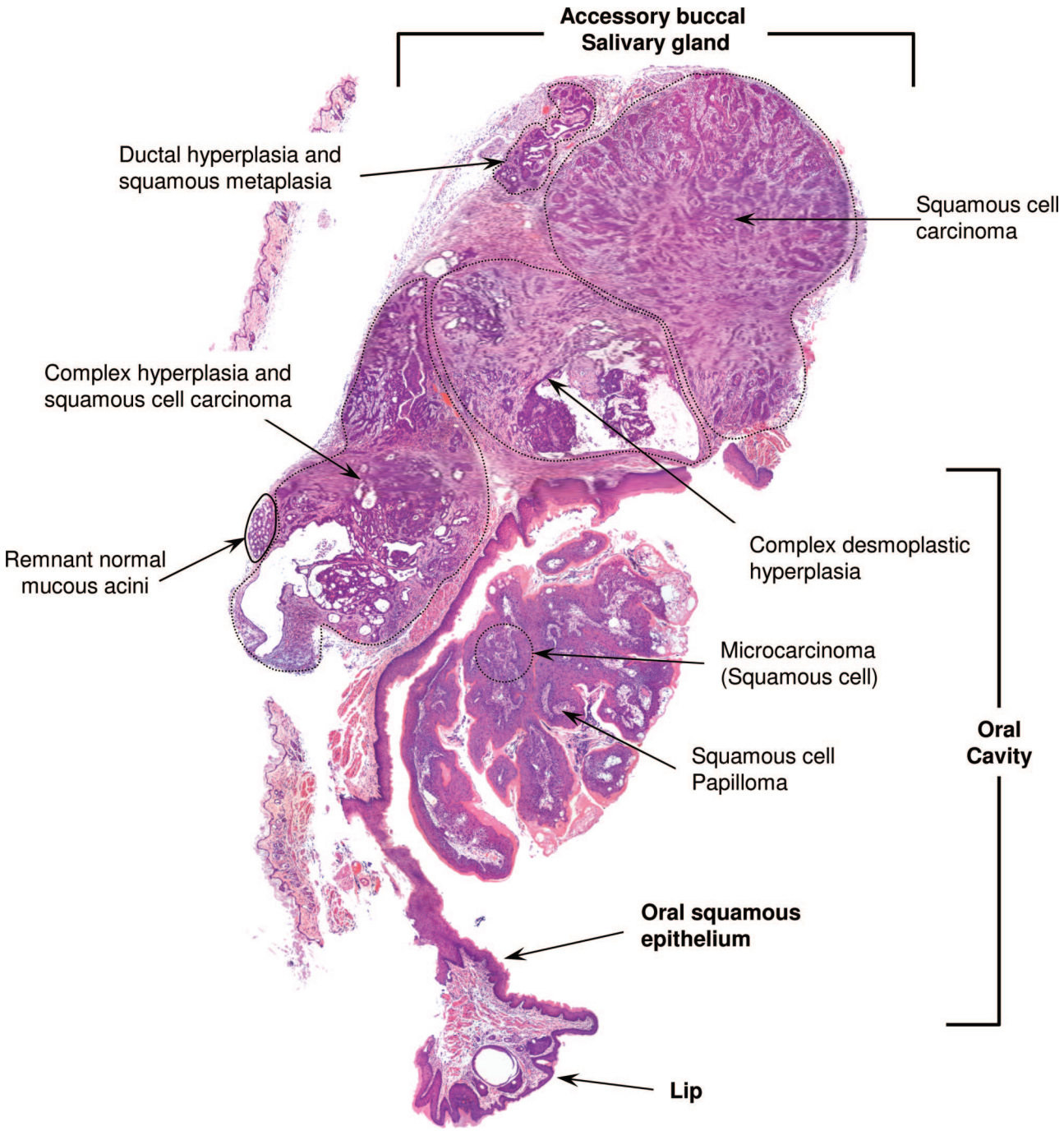

Figure 5. Panoramic view of a buccal accessory salivary gland with a wide spectrum of histological changes from hyperplasia to carcinoma, showing its relations with the oral cavity. Note that, unlike the extraorbital lacrimal glands, these structures contain mucous acini, remnants of which are shown. A squamous papilloma of the oral epithelium that has an area of invasive carcinoma can also be seen. Magnification: ×40.

of basal cells in all salivary gland ducts (Figure 6, B–D). The submaxillary gland (Figure 6D) showed a higher number of positive structures as compared with the sublingual gland (Figure 6C); the myoepithelial cells were also immunoreactive for K5 in both glands. Double β-galactosidase/K5 staining confirmed that all cells expressing the transgene were K5-positive (data not shown). Furthermore, immunostaining of hyperplastic and dysplastic lesions revealed that the hyperproliferating cells arose from the K5-positive cell compartment (Figures 6E, 7, A and B). In carcinomas, K5 expression varied on tumor differentiation. Almost all cells were positive in moderately differentiated carcinomas, whereas in spindle-shaped tumors, as well as in metastases, expression could be patchy (Figure 7C and inset). Immunostaining for smooth muscle actin showed the participation of myoepithelial cells in the stromal alterations accompanying hyperplasias and dysplasias, mainly in the submaxillary gland. Myoepithelial cells were identified intermingled with proliferating cells and in the periphery of neoplastic nodules (Figure 7E, arrows). They were not, how-

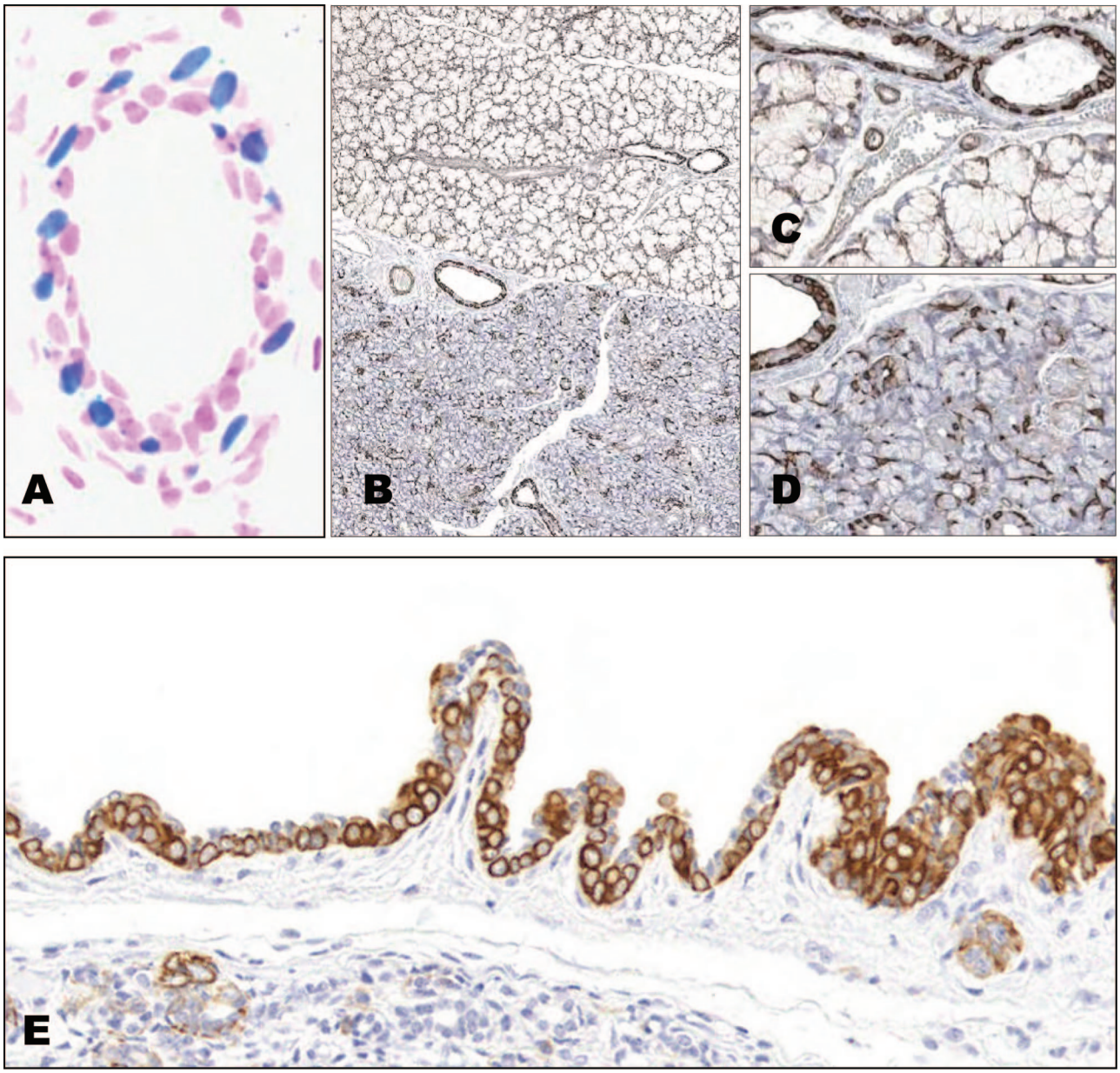

Figure 6. A: β-Galactosidase staining; isolated ductal cells are positive. **B:** Immunostaining for keratin 5 in sublingual (upper figure) and submaxillary (lower figure) glands reveals positive staining in most ductal cells as well as in myoepithelial cells. **C:** Higher magnification of K5 expression in the sublingual gland. **D:** Submaxillary gland immunoreacted with K5. **E:** K5-*tet*-on/*tet*-o-*ras* mice. K5 is expressed in all proliferating cells in a hyperplastic excretory duct. Magnifications: ×40 (**B**); ×60 (**C–E**); and ×120 (**A**).

ever, a component of the carcinoma, because neoplastic cells were smooth muscle actin-negative (Figure 7, D and E). p53 staining was negative in all dysplasias and tumors examined, suggesting that alterations leading to the accumulation of this gene product may not be part of the mechanisms of carcinogenesis in this model. *p63* was positive mainly in the cell nuclei in proliferating areas, and both benign and carcinomatous areas showed a higher percentage of stained cells (Figure 7H, Ca: carcinoma; Hyp: hyperplastic area) as compared within normal tissues in which only scattered cells reacted (Figure 7, F and G). Carcinomas exhibited a higher percentage of *p63*-positive cells when compared with hyperplastic or dysplastic epithelial areas. Myoepithelial cells as well as stromal cells were negative for *p63*. Few cells incorporated BrdU in normal salivary glands, and the proportion of BrdU-immunoreactive cells in BrdU-treated control animals was usually higher in ductal structures as compared with acini. In contrast, a remarkable increase in cell proliferation was evident in early lesions as well as in tumor areas of *ras*-expressing animals (Figure 7, I and J, arrows: normal tissue; empty arrows: proliferative areas).

Discussion

We have developed a mouse model system that enables the study of the carcinogenic process in salivary glands

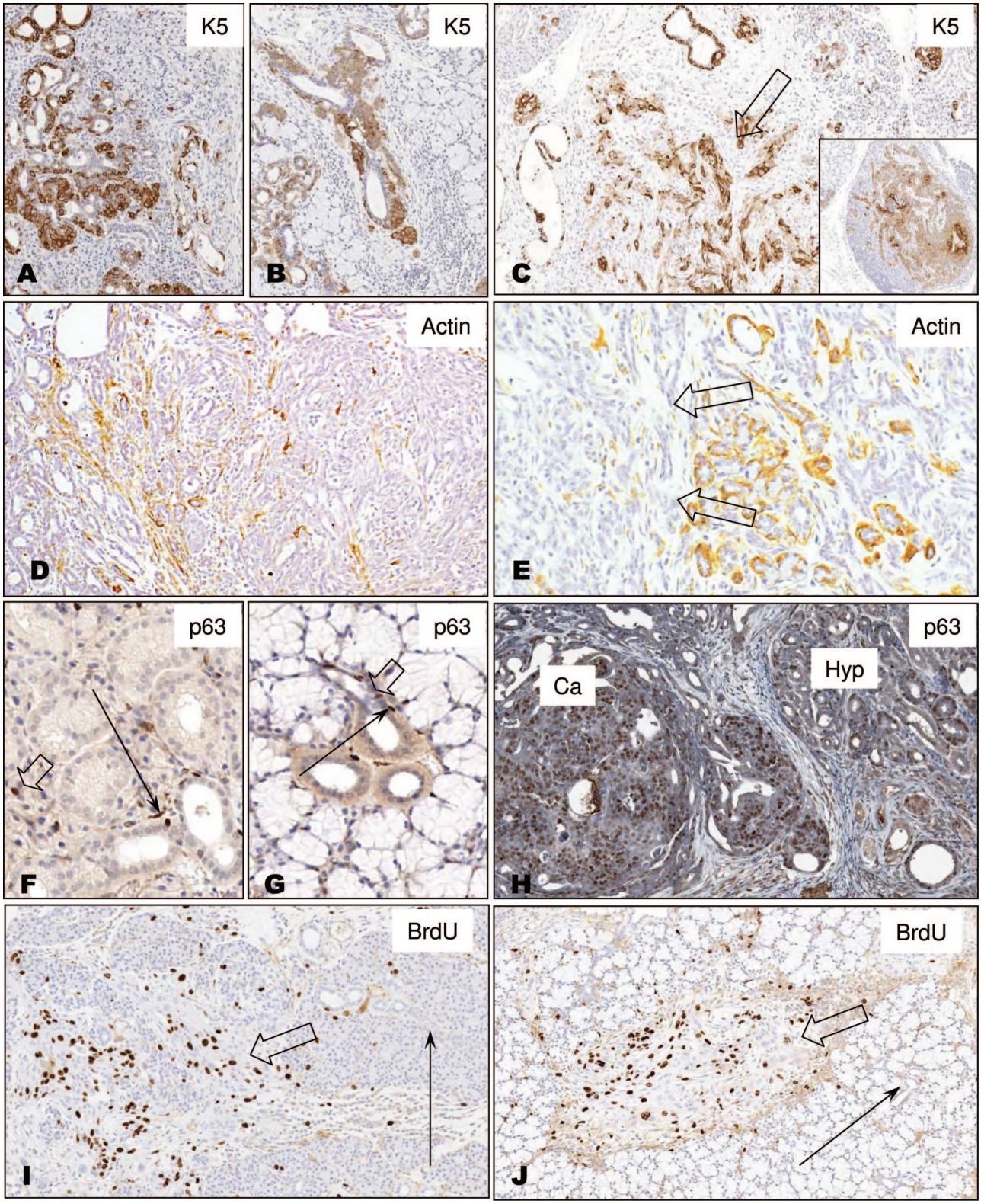

Figure 7. A and **B:** K5 staining in the hyperplastic area of the submaxillary and sublingual glands, respectively, showing strong immunoreactivity in the proliferating cells. **C:** Strong K5 immunoreactivity in carcinomatous cells (**arrow**), as well as in a lymph node metastasis (**inset**). **D:** Distribution of smooth muscle actin staining in a dysplasia, with scattered cells surrounding glandular structures. In **E**, the carcinomatous area on the left side of the picture is negative (**arrows**), whereas the hyperplastic glands on the right side show positive periglandular myoepithelial cells. **F** and **G:** Scattered immunoreactivity for p63 in normal submaxillary and sublingual glands respectively (**empty arrows**: ductal cells; **arrows**: myoepithelial cells). In **H**, a higher number of p63-immunoreactive cells are seen in the carcinomatous (Ca) as compared with a hyperplastic area (Hyp). In both cases the proportion of positive cells is higher than that of normal tissues. **I** and **J:** a higher proportion of BrdU-retaining cells in hyperplastic areas (**empty arrows**) as compared with normal areas (**arrows**) in submaxillary and sublingual glands, respectively. Magnifications: ×30 (**A–C**); ×40 (**D**, **E**, **H**, **I**, and **J**); and ×60 (**F** and **G**).

by targeting the conditional expression of a mutant *ras* oncogene in a highly susceptible cell compartment in the salivary glands. Previously available transgenic animal models targeting the expression of a variety of oncogenes to the salivary glands are characterized by their high latency and low incidence of salivary gland tumors. Indeed, enhanced conversion to malignancy often requires the expression of more than one oncogene, or oncogene expression in mice deficient in a tumor suppressor gene. As such, coexpression of MMTV-v-Ha-*ras* and MMTV-c-*myc* genes[24] or MMTV-c-*myc* and MMTV-TGFα[25] act in a synergistic fashion, and double transgenic mice develop several malignancies within months, including adenocarcinomas of parotid gland. MMTV-c-*neu* mice do not display any salivary gland abnormalities, but when both alleles of *p53* are inactivated, the majority of the animals develop parotid gland tumors by 16 weeks of age.[26] Tumors also developed, albeit to a lesser extent, in p53 heterozygous animals harboring only one functional *p53* gene.[26]

The fact that most proliferative lesions in the K5-*tet*-on/*tet-ras* model seem to proceed through squamous metaplasia may be interpreted as this process being triggered by this specific oncogene or the cell compartment in which the K5 promoter is expressed being composed of reserve cells already committed to differentiate into squamous epithelium. In this regard, squamous metaplasia has been previously described as a feature of other experimental models involving *ras* mutations in organs with glandular epithelium, such as in *N*-methyl-*N*-nitrosourea-induced mammary carcinogenesis,[27,28] so it is possible that *ras* may stimulate signal transduction pathways promoting squamous differentiation as part of the carcinogenic process. On the other hand, squamous metaplasia represents an adaptative, reversible response of nonsquamous epithelia to an environmental change.[22] It proceeds through a series of histologically identifiable steps from basal cell hyperplasia to eventual maturation to full squamous epithelium. The signal transduction pathways and biochemical changes underlying this phenomenon are still poorly understood. In our model, unlike what normally happens in epidermal differentiation in which irreversible growth arrest is an early event as cells transit from the basal to the suprabasal layers, full induction of differentiation-specific genes is hampered due to the K5 promoter-driven expression of *ras*. The epithelium never reaches full differentiation as evidenced by the absence of clear keratinization, thus resulting in squamous metaplasia. Proliferation is uncoupled from differentiation in this model, possibly accounting for the rapid development of carcinomas.

One of the most striking features of this model is the fast onset and high incidence of tumor development. In this conditional transgenic animal system, the *ras* oncogene may be targeted to a salivary gland compartment composed of reserve cells already committed to differentiate into squamous epithelium. Because they retain a full proliferative capacity and by definition constitute the less differentiated/committed compartment, they may be vulnerable to rapid oncogenic transformation. As we have previously discussed,[20] recently developed mathematical models suggest that small populations of stem cells harboring mutations may accumulate during development; these cell populations, although not tumorigenic in nature, may predispose to certain late-life cancers, because they may not require the accumulation of additional mutations subsequent to *ras* activation for malignant conversion.[29] This may help us understand the fast and multifocal neoplastic growth in this model.

It is also interesting that p53 immunostaining was negative across all carcinomatous lesions, a staining pattern associated with lack of p53 accumulation, thus suggesting that mutations resulting in the inactivation and stabilization of this important tumor suppressor gene product may not be necessary for carcinogenesis to proceed. On the other hand, these observations do not preclude the possibility that p53 can harbor mutations that do not result in its stabilization, or that p53 function may be inhibited by epigenetic events, such as by enhancing its degradation or by interference with proteins controlling its transcriptional activity. In this setting it is interesting to speculate the possibility that *ras* expression in a compartment that includes the salivary gland stem cells is sufficient to trigger the acquisition of an oncogenic and metastatic phenotype without requiring a multistep process involving the accumulation of mutations in p53. Further studies will be necessary to explore this possibility. Alternatively, *ras* may inhibit p53 function by a still not fully understood mechanism. This could include the contribution of the *p63* gene, a member of the p53 family that can inhibit p53 function and that is expressed in normal and neoplastic basal and myoepithelial cells of the salivary glands,[30,31] squamous cell carcinomas of the oral cavity,[32] as well as in a variety of other normal and tumor tissues.[33] Indeed, we have observed a highly elevated expression of the ΔN isoform of *p63* in *ras*-induced salivary gland tumors as compared to normal and non-neoplastic tissues, and this splice variant of *p63* can inhibit p53 transcriptional activity.[34]

The highly proliferative nature of salivary gland tumors induced by *ras* was further demonstrated by BrdU incorporation, which is evidently higher in tumors as compared with hyperplastic/dysplastic and normal tissues. A conspicuous absentee in these tumors is the stroma. Only in the very advanced cases of carcinomas did we find alterations usually associated with a stromal reaction, namely fibrosis, leukocyte infiltration, and vessel proliferation. An unexpected finding obtained while characterizing this model has been the identification of a group of accessory buccal salivary glands. This is not surprising, however, because they are microscopic and are evident only after a careful dissection of the tissues surrounding the mouth angle. Their rapid tumoral growth is an interesting feature of the salivary gland phenotype elicited by doxycycline treatment of K5-*tet*-on/*tet-ras* animals, because these accessory glands were affected with latency as short as that of the major salivary glands. The fact that they are contiguous with the buccal mucosa, which is exposed to high concentrations of dietary doxycycline, may account for their rapid and constant involvement.

In summary, we describe here a novel model of salivary gland carcinogenesis in which the conditional ex-

pression of a mutated *ras* oncogene in salivary gland tissues under the control of the K5 promoter results in complete carcinogenesis with a minimum latency of 7 days. Some critical aspects of this model, such as the apparent absence of recognizable preneoplastic events in some of the carcinomas, raises the possibility of the existence of a subset of highly susceptible cells within the salivary gland that may be prone to oncogenic conversion. These cells are likely to reside in the epithelium underlying the salivary gland ducts, within the stem cell compartment. The full identification of the cell of origin of the tumors arising in this animal model, as well as the likely possibility that this particular cell population might contribute to human malignancies of the salivary glands, warrants further investigation.

References

1. Speight PM, Barrett AW: Salivary gland tumours. Oral Dis 2002, 8:229–240
2. Dardick I. Color Atlas/Text of Salivary Gland Tumor Pathology, New York, Igaku-Shoin Medical Publisher, Inc., 1996
3. Histological Typing of Salivary Gland Tumours. World Health Organization International histological classification of tumours, New York, TELOS, Springer-Verlag, 1991
4. Ellis GL, Auclair PL: Atlas of tumor pathology. Tumors of the salivary glands, Washington, DC, Armed Forces Institute of Pathology, 1996, p 31
5. Ide F, Suka N, Kitada M, Sakashita H, Kusama K, Ishikawa T: Skin and salivary gland carcinogenicity of 7,12-dimethylbenz[*a*]anthracene is equivalent in the presence or absence of aryl hydrocarbon receptor. Cancer Lett 2004, 214:35–41
6. Azuma M, Tamatani T, Kasai Y, Sato M: Immortalization of normal human salivary gland cells with duct-, myoepithelial-, acinar-, or squamous phenotype by transfection with SV40 ori- mutant deoxyribonucleic acid. Lab Invest 1993, 69:24–42
7. Espinal EG, Ubios AM, Cabrini RL: Salivary gland tumors induced by 32P. J Oral Pathol 1984, 13:686–691
8. Dardick I, Ho J, Paulus M, Mellon PL, Mirels L: Submandibular gland adenocarcinoma of intercalated duct origin in Smgb-Tag mice. Lab Invest 2000, 80:1657–1670
9. Tsukamoto AS, Grosschedl R, Guzman RC, Parslow T, Varmus HE: Expression of the int-1 gene in transgenic mice is associated with mammary gland hyperplasia and adenocarcinomas in male and female mice. Cell 1988, 55:619–625
10. Jhappan C, Gallahan D, Stahle C, Chu E, Smith GH, Merlino G, Callahan R: Expression of an activated Notch-related int-3 transgene interferes with cell differentiation and induces neoplastic transformation in mammary and salivary glands. Genes Dev 1992, 6:345–355
11. Daphna-Iken D, Shankar DB, Lawshe, Ornitz DM, Shackleford GM, MacArthur CA: MMTV-Fgf8 transgenic mice develop mammary and salivary gland neoplasia and ovarian stromal hyperplasia. Oncogene 1998, 17:2711–2717
12. Dardick I, Burford-Mason AP, Garlick DS, Carney WP: The pathobiology of salivary gland. II. Morphological evaluation of acinic cell carcinomas in the parotid gland of male transgenic (MMTV/v-Ha-ras) mice as a model for human tumours. Virchows Arch A Pathol Anat Histopathol 1992, 421:105–113
13. Rodenhuis S: ras and human tumors. Semin Cancer Biol 1992, 3:241–247
14. Milasin J, Pujic N, Dedovic N, Gavric M, Vranik V, Petrovic V, Minic A: H-ras gene mutations in salivary gland pleomorphic adenomas. Int J Oral Maxillofac Surg 1993, 22:359–361
15. Stenman G, Sandros J, Mark J, Nordkvist A: High p21RAS expression levels correlate with chromosome 8 rearrangements in benign human mixed salivary gland tumors. Genes Chromosomes Cancer 1989, 1:59–66
16. Zachos G, Spandidos DA: Expression of ras proto-oncogenes: regulation and implications in the development of human tumors. Crit Rev Oncol Hematol 1997, 26:65–75
17. van Halteren HK, Top B, Mooi WJ, Balm AJ, Rodenhuis S: Association of H-ras mutations with adenocarcinomas of the parotid gland. Int J Cancer 1994, 57:362–364
18. Andres AC, Schonenberger CA, Groner B, Hennighausen L, LeMeur M, Gerlinger P: Ha-ras oncogene expression directed by a milk protein gene promoter: tissue specificity, hormonal regulation, and tumor induction in transgenic mice. Proc Natl Acad Sci USA 1987, 84:1299–1303
19. Schaffner DL, Barrios R, Shaker MR, Rajagopalan S, Huang SL, Tindall DJ, Young CY, Overbeek PA, Lebovitz RM, Lieberman MW: Transgenic mice carrying a PSArasT24 hybrid gene develop salivary gland and gastrointestinal tract neoplasms. Lab Invest 1995, 72:283–290
20. Vitale-Cross L, Amornphimoltham P, Fisher G, Molinolo AA, Gutkind JS: Conditional expression of K-ras in an epithelial compartment that includes the stem cells is sufficient to promote squamous cell carcinogenesis. Cancer Res 2004, 64:8804–8807
21. Ramirez A, Bravo A, Jorcano JL, Vidal M: Sequences 5′ of the bovine keratin 5 gene direct tissue- and cell-type-specific expression of a lacZ gene in the adult and during development. Differentiation 1994, 58:53–64
22. Robbins & Cotran Pathologic Basis of Disease, Philadelphia, W. B. Saunders, 2004 (hardcover)
23. The Staff of the Jackson Laboratory. Biology of the Laboratory Mouse, Dover Publications, Inc., New York, 1981
24. Sinn E, Muller W, Pattengale P, Tepler I, Wallace R, Leder P: Coexpression of MMTV/v-Ha-*ras* and MMTV/c-*myc* genes in transgenic mice: synergistic action of oncogenes in vivo. Cell 1987, 49:465–475
25. Amundadottir LT, Johnson MD, Merlino G, Smith GH, Dickson RB: Synergistic interaction of transforming growth factor alpha and c-*myc* in mouse mammary and salivary gland tumorigenesis. Cell Growth Differ 1995, 6:737–748
26. Brodie SG, Xu X, Li C, Kuo A, Leder P, Deng CX: Inactivation of p53 tumor suppressor gene acts synergistically with c-*neu* oncogene in salivary gland tumorigenesis. Oncogene 2001, 20:1445–1454
27. Miyamoto S, Guzman RC, Osborn RC, Nandi S: Neoplastic transformation of mouse mammary epithelial cells by in vitro exposure to *N*-methyl-*N*-nitrosourea. Proc Natl Acad Sci USA 1988, 85:477–481
28. Pazos P, Lanari C, Elizalde P, Montecchia F, Charreau EH, Molinolo AA: Promoter effect of medroxyprogesterone acetate (MPA) in *N*-methyl-N-nitrosourea (MNU) induced mammary tumors in BALB/c mice. Carcinogenesis 1998, 19:529–531
29. Frank SA, Nowak MA: Cell biology: developmental predisposition to cancer. Nature 2003, 422:494
30. Bilal H, Handra-Luca A, Bertrand JC, Fouret PJ: P63 is expressed in basal and myoepithelial cells of human normal and tumor salivary gland tissues. J Histochem Cytochem 2003, 51:133–139
31. Seethala RR, Livolsi VA, Zhang PJ, Pasha TL, Baloch ZW: Comparison of p63 and p73 expression in benign and malignant salivary gland lesions. Head Neck 2005, 27:696–702
32. Foschini MP, Gaiba A, Cocchi R, Pennesi MG, Gatto MR, Frezza GP, Pession A: Pattern of p63 expression in squamous cell carcinoma of the oral cavity. Virchows Arch 2004, 444:332–339
33. Reis-Filho JS, Simpson PT, Martins A, Preto A, Gartner F, Schmitt FC: Distribution of p63, cytokeratins 5/6 and cytokeratin 14 in 51 normal and 400 neoplastic human tissue samples using TARP-4 multi-tumor tissue microarray. Virchows Arch 2003, 443:122–132
34. Yang A, Kaghad M, Wang Y, Gillett E, Fleming MD, Dotsch V, Andrews NC, Caput D, McKeon F: p63, a p53 homolog at 3q27–29, encodes multiple products with transactivating, death-inducing, and dominant-negative activities. Mol Cell 1998, 2:305–316